Dynamic Neural Network-Based Output Feedback Tracking Control for Uncertain Nonlinear Systems

Huyen T. Dinh[1]
Department of Mechanical Engineering,
University of Transport and Communications,
Hanoi, Vietnam
e-mail: huyentdinh@utc.edu.vn

S. Bhasin
Department of Electrical Engineering,
Indian Institute of Technology,
Delhi, India
e-mail: sbhasin@ee.iitd.ac.in

R. Kamalapurkar
School of Mechanical and Aerospace Engineering,
Oklahoma State University,
Stillwater, OK 74074
e-mail: rushikesh.kamalapurkar@okstate.edu

W. E. Dixon
Department of Mechanical and Aerospace Engineering,
University of Florida,
Gainesville, FL 32611
e-mail: wdixon@ufl.edu

A dynamic neural network (DNN) observer-based output feedback controller for uncertain nonlinear systems with bounded disturbances is developed. The DNN-based observer works in conjunction with a dynamic filter for state estimation using only output measurements during online operation. A sliding mode term is included in the DNN structure to robustly account for exogenous disturbances and reconstruction errors. Weight update laws for the DNN, based on estimation errors, tracking errors, and the filter output are developed, which guarantee asymptotic regulation of the state estimation error. A combination of a DNN feedforward term, along with the estimated state feedback and sliding mode terms yield an asymptotic tracking result. The developed output feedback (OFB) method yields asymptotic tracking and asymptotic estimation of unmeasurable states for a class of uncertain nonlinear systems with bounded disturbances. A two-link robot manipulator is used to investigate the performance of the proposed control approach. [DOI: 10.1115/1.4035871]

1 Introduction

The problem of output feedback (OFB) tracking control for nonlinear dynamic systems has been a topic of considerable interest over the past several decades. Motivation arises from the fact that full access to system states is sometimes impossible in many practical systems. An obvious method to estimate the unmeasurable states is using *ad hoc* numerical differentiation. The simplicity of this technique makes it particularly useful for implementation. However, if output measurements are noisy, such numerical techniques will amplify the high frequency content which may produce undesired oscillations or even system instability. Other solutions can be classified as observer-based or filter-based techniques that utilize the output information for estimating unmeasurable states. While observers estimate the output derivative by approximating the system dynamics, filters approximate the behavior of a differentiator over a range of frequencies. Hence, observer designs need partial or exact model knowledge of the system dynamics, whereas filters can provide a model-free means of estimating unmeasurable states.

Output feedback controllers using model-based observers were developed in Refs. [1–4], based on the assumption of exact model knowledge. OFB control for systems with parametric uncertainties have been developed in Refs. [5–7]. However, a limitation of such previous adaptive OFB control approaches is that only linear-in-the-parameters (LP) uncertainties are considered. As a result, if uncertainties in the system do not satisfy the LP condition or if the system is affected by disturbances, the results will reduce to a uniformly ultimately bounded result.

Neural network (NN) and fuzzy logic are employed to compensate adaptively for the uncertainties to relax the LP condition as in Refs. [8–14]; however, both estimation and tracking errors are only guaranteed to be bounded due to the existence of reconstruction errors. A semiglobal asymptotic OFB tracking result for second-order dynamic systems, under the condition that uncertain dynamics are first-order differentiable, was developed in Ref. [15] using a novel filter design. All of the uncertain nonlinearities in Ref. [15] are damped out by a sliding mode term, so the discontinuous controller requires high-gain. However, it is not clear how to simply add a NN-based feedforward estimation of the nonlinearities in results such as Ref. [15] to mitigate the high-gain condition, because of the need to inject nonlinear functions of the unmeasurable state. The approach used in this paper avoids this issue by exploiting the recurrent nature of a dynamic neural network (DNN) structure to inject terms that cancel cross terms in the stability analysis associated with the unmeasurable state.

In this paper and the preliminary work in Ref. [16], a DNN-based observer-controller is proposed for uncertain nonlinear systems affected by bounded disturbances, to achieve a two-fold result: asymptotic estimation of the unmeasurable states and asymptotic tracking control. The uncertain dynamics are assumed to be first-order differentiable. The universal approximation property of DNNs is utilized to approximate the uncertain nonlinear system. A modified version of the filter introduced in Ref. [15] is used to estimate the output derivative. A combination of a NN feedforward term, along with estimated state feedback and sliding mode terms are designed for the controller. The DNN observer adapts online for nonlinear uncertainties and should heuristically perform better than a robust feedback observer. Weight update laws for the DNN based on the estimation error, tracking error, and filter output are proposed. Asymptotic regulation of the estimation error and asymptotic tracking are achieved. Experiments on a two-link robot manipulator show the effectiveness of the developed method compared with a proportional–integral–derivative (PID) controller and the approach in Ref. [15].

2 System Model and Objectives

Consider a control-affine second-order Euler–Lagrangelike nonlinear system of the form

$$\ddot{x} = f(x, \dot{x}) + G(x)u + d \tag{1}$$

where $x \in \mathbb{R}^n$ is the measurable output with a finite-initial condition $x(0) = x_0$, $u \in \mathbb{R}^n$ is the control input, $f : \mathbb{R}^{2n} \to \mathbb{R}^n$ and $G : \mathbb{R}^n \to \mathbb{R}^{n\times n}$ are continuous functions, and $d(t) \in \mathbb{R}^n$ is an exogenous disturbance. The following assumptions about the system in Eq. (1) will be utilized in the subsequent development.

Assumption 1. *The time derivatives of the system output $\dot{x}$, $\ddot{x}$ are not measurable.*

Assumption 2. *The unknown function f is C^1, and the function G is known, invertible, and the matrix inverse G^{-1} is bounded.*

[1]Corresponding author.

Contributed by the Dynamic Systems Division of ASME for publication in the Journal of Dynamic Systems, Measurement, and Control. Manuscript received May 3, 2016; final manuscript received January 20, 2017; published online May 10, 2017. Assoc. Editor: Yongchun Fang.

Assumption 3. *The nonlinear disturbance d and its first time derivative are bounded (i.e., $d,\ \dot{d} \in \mathcal{L}_\infty$).*

The universal approximation property of multilayer NNs (MLNN) states that given any continuous function $F : \mathbb{S} \to \mathbb{R}^n$, where $\mathbb{S}$ is a compact set, there exist ideal weights such that the output of the NN, $\hat{F}$ approximates F to an arbitrary accuracy [17,18]. Hence, the unknown function f in Eq. (1) can be replaced by a MLNN, and the system can be represented as

$$\ddot{x} = W^{\mathrm{T}}\sigma(V_1^{\mathrm{T}}x + V_2^{\mathrm{T}}\dot{x}) + \varepsilon(x,\dot{x}) + Gu + d \tag{2}$$

where $W \in \mathbb{R}^{N+1\times n}$, $V_1, V_2 \in \mathbb{R}^{n\times N}$ are unknown ideal constant weight matrices of the MLNN having N hidden layer neurons, $\sigma \triangleq \sigma(V_1^{\mathrm{T}}x + V_2^{\mathrm{T}}\dot{x}) : \mathbb{R}^{2n} \to \mathbb{R}^{N+1}$ is the activation function (sigmoid, hyperbolic tangent, etc.), and $\varepsilon \in \mathbb{R}^n$ is a function reconstruction error. The following assumptions will be used in the DNN-based observer and controller development and stability analysis.

Assumption 4. *The ideal NN weights are bounded by known positive constants [19], i.e., $||W|| \le \overline{W}$, $||V_1|| \le \overline{V}_1$, $||V_2|| \le \overline{V}_2$.*

Assumption 5. *The activation function σ and its partial derivatives σ', σ'' are bounded [19]. This assumption is satisfied for typical activation functions (e.g., sigmoid, hyperbolic tangent).*

Assumption 6. *The function reconstruction error and its first time derivative are bounded [19], as $||\varepsilon|| \le \bar{\varepsilon}_1$, $||\dot{\varepsilon}|| \le \bar{\varepsilon}_2$, where $\bar{\varepsilon}_1, \bar{\varepsilon}_2$ are known positive constants.*

A contribution of this paper is the development of a robust DNN-based observer such that the estimated states asymptotically converge to the real states of the system (1), and a discontinuous controller enables the system state to asymptotically track a desired time-varying trajectory $x_d \in \mathbb{R}^n$, despite uncertainties and disturbances in the system. To quantify these objectives, an estimation error $\tilde{x} \in \mathbb{R}^n$ and a tracking error $e \in \mathbb{R}^n$ are defined as

$$\tilde{x} \triangleq x - \hat{x}, \quad e \triangleq x - x_d \tag{3}$$

where $\hat{x} \in \mathbb{R}^n$ is the state of the DNN observer which is introduced in the subsequent development. The desired trajectory x_d and its derivatives $x_d^{(i)}$ $(i = 1, 2)$, are assumed to exist and be bounded. To compensate for the lack of direct measurements of $\dot{x}$, a filtered estimation error, $r_{\mathrm{es}} \in \mathbb{R}^n$, and a filtered tracking error, $r_{\mathrm{tr}} \in \mathbb{R}^n$, are defined as

$$r_{\mathrm{es}} \triangleq \dot{\tilde{x}} + \alpha\tilde{x} + \eta, \quad r_{\mathrm{tr}} \triangleq \dot{e} + \alpha e + \eta \tag{4}$$

where $\alpha \in \mathbb{R}$ is a positive constant gain, and $\eta \in \mathbb{R}^n$ is an output of the dynamic filter

$$\begin{aligned} \eta &= p - (k+\alpha)\tilde{x} \\ \dot{p} &= -(k+2\alpha)p - \nu + ((k+\alpha)^2 + 1)\tilde{x} + e \\ \dot{\nu} &= p - \alpha\nu - (k+\alpha)\tilde{x},\ \ p(0) = (k+\alpha)\tilde{x}(0),\ \ \nu(0) = 0 \end{aligned} \tag{5}$$

where $\nu \in \mathbb{R}^n$ is another output of the filter, $p \in \mathbb{R}^n$ is used as an internal filter variable, and $k \in \mathbb{R}$ is a positive constant control gain. The filtered estimation error r_{es} and the filtered tracking error r_{tr} are not measurable since the expressions in Eq. (4) depend on $\dot{x}$.

Remark 1. The basic structure of the second-order dynamic filter in Eq. (5) was first proposed in Eq. [15]. The filter in Eq. (5) admits the estimation error $\tilde{x}$ and the tracking error e as its inputs and produces two signal outputs ν and η. An interesting point is that there is a virtual filter inside the introduced filter, where η is the filtered signal of ν since η and ν are related as $\eta = \dot{\nu} + \alpha\nu$. The auxiliary signal p is utilized to only generate the signal η without involving the unmeasurable state $\dot{x}$. Hence, the filter can be physically implemented since it depends only on the estimation error $\tilde{x}$ and the tracking error e which are measurable.

3 Dynamic Neural Network-Based Robust Observer

The following MLDNN architecture is proposed to observe the system in Eq. (1)

$$\ddot{\hat{x}} = \hat{W}^{\mathrm{T}}\hat{\sigma} + \mathrm{Gu} - (k+3\alpha)\eta + \beta_1\mathrm{sgn}(\tilde{x} + \nu) \tag{6}$$

where $[\hat{x}^{\mathrm{T}}\ \dot{\hat{x}}^{\mathrm{T}}]^{\mathrm{T}} \in \mathbb{R}^{2n}$ are the states of the DNN observer, $\hat{W} \in \mathbb{R}^{N+1\times n}$, $\hat{V}_1, \hat{V}_2 \in \mathbb{R}^{n\times N}$ are the weight estimates, $\hat{\sigma} \triangleq \sigma(\hat{V}_1^{\mathrm{T}}\hat{x} + \hat{V}_2^{\mathrm{T}}\dot{\hat{x}}) : \mathbb{R}^{2n} \to \mathbb{R}^{N+1}$, and $\beta_1 \in \mathbb{R}$ is a positive constant control gain.

Remark 2. The term $(k+3\alpha)\eta$ in the DNN observer in Eq. (6) is a cross-term which is canceled in the stability analysis. The sliding mode term $\mathrm{sgn}(\tilde{x}+\nu)$ is added to the observer structure to provide robustness against NN reconstruction errors and external disturbances. The NN term $\hat{W}^{\mathrm{T}}\hat{\sigma}$ receives feedback of the observer states $\hat{x}, \dot{\hat{x}}$ as inputs; hence the observer exploits a DNN structure. Motivation for the DNN-based observer design is that the DNN is proven to approximate nonlinear dynamic systems with any degree of accuracy [17,20], and the DNN includes state feedback yielding computational advantages over a static feedforward NN [21].

The weight update laws for the DNN in (6) are developed based on the subsequent stability analysis as

$$\begin{aligned} \dot{\hat{W}} &= \Gamma_w \mathrm{proj}[\hat{\sigma}_d(\tilde{x} + e + 2\nu)^{\mathrm{T}}] \\ \dot{\hat{V}}_1 &= \Gamma_{v1}\mathrm{proj}[x_d(\tilde{x} + e + 2\nu)^{\mathrm{T}}\hat{W}^{\mathrm{T}}\hat{\sigma}'_d] \\ \dot{\hat{V}}_2 &= \Gamma_{v2}\mathrm{proj}[\dot{x}_d(\tilde{x} + e + 2\nu)^{\mathrm{T}}\hat{W}^{\mathrm{T}}\hat{\sigma}'_d] \end{aligned} \tag{7}$$

where $\Gamma_w \in \mathbb{R}^{(N+1)\times(N+1)}$, $\Gamma_{v1}, \Gamma_{v2} \in \mathbb{R}^{n\times n}$, are constant symmetric positive-definite adaptation gains, the terms $\hat{\sigma}_d, \hat{\sigma}'_d$ are defined as $\hat{\sigma}_d \triangleq \sigma(\hat{V}_1^{\mathrm{T}}x_d + \hat{V}_2^{\mathrm{T}}\dot{x}_d)$, $\hat{\sigma}'_d \triangleq d\sigma(\varsigma)/d\varsigma|_{\varsigma = \hat{V}_1^{\mathrm{T}}x_d + \hat{V}_2^{\mathrm{T}}\dot{x}_d}$, and $\mathrm{proj}(\cdot)$ is a smooth projection operator [22,23] used to guarantee that the weight estimates $\hat{W}, \hat{V}_1, \hat{V}_2$ remain bounded.

To facilitate the subsequent analysis, Eqs. (4) and (5) can be used to express the time derivative of η as

$$\dot{\eta} = -(k+\alpha)r_{\mathrm{es}} - \alpha\eta + \tilde{x} + e - \nu \tag{8}$$

The closed-loop dynamics of the filtered estimation error in Eq. (4) can be determined by using Eqs. (2)–(4), (6), and (8) as

$$\begin{aligned} \dot{r}_{\mathrm{es}} &= W^{\mathrm{T}}\sigma - \hat{W}^{\mathrm{T}}\hat{\sigma} + \varepsilon + d + (k+3\alpha)\eta - \beta_1\mathrm{sgn}(\tilde{x}+\nu) \\ &\quad + \alpha(r_{\mathrm{es}} - \alpha\tilde{x} - \eta) - (k+\alpha)r_{\mathrm{es}} - \alpha\eta + \tilde{x} + e - \nu \end{aligned} \tag{9}$$

Adding and subtracting $W^{\mathrm{T}}\sigma_d + W^{\mathrm{T}}\hat{\sigma}_d + \hat{W}^{\mathrm{T}}\hat{\sigma}_d$, where $\sigma_d \triangleq \sigma(V_1^{\mathrm{T}}x_d + V_2^{\mathrm{T}}\dot{x}_d)$, the expression in Eq. (9) can be rewritten as

$$\dot{r}_{\mathrm{es}} = \tilde{N}_1 + N - kr_{\mathrm{es}} - \beta_1\mathrm{sgn}(\tilde{x}+\nu) + (k+\alpha)\eta - \tilde{x} \tag{10}$$

where the auxiliary term $\tilde{N}_1 \in \mathbb{R}^n$ is defined as

$$\tilde{N}_1 \triangleq W^{\mathrm{T}}(\sigma - \sigma_d) - \hat{W}^{\mathrm{T}}(\hat{\sigma} - \hat{\sigma}_d) - (\alpha^2 - 2)\tilde{x} - \nu + e \tag{11}$$

and $N \in \mathbb{R}^n$ is segregated into two parts as

$$N \triangleq N_D + N_B \tag{12}$$

In Eq. (12), N_D, $N_B \in \mathbb{R}^n$ are defined as

$$N_D \triangleq \varepsilon + d, \quad N_B \triangleq N_{B_1} + N_{B_2} \tag{13}$$

In Eq. (13), $N_{B_1}, N_{B_2} \in \mathbb{R}^n$ are defined as

$$\begin{aligned} N_{B_1} &\triangleq W^{\mathrm{T}} O(\tilde{V}_1^{\mathrm{T}} x_d + \tilde{V}_2^{\mathrm{T}} \dot{x}_d)^2 + \tilde{W}^T \hat{\sigma}_d'(\tilde{V}_1^{\mathrm{T}} x_d + \tilde{V}_2^{\mathrm{T}} \dot{x}_d) \\ N_{B_2} &\triangleq \tilde{W}^{\mathrm{T}} \hat{\sigma}_d + \hat{W}^{\mathrm{T}} \hat{\sigma}_d'(\tilde{V}_1^{\mathrm{T}} x_d + \tilde{V}_2^{\mathrm{T}} \dot{x}_d) \end{aligned} \tag{14}$$

where $\tilde{W} \triangleq W - \hat{W} \in \mathbb{R}^{N+1 \times n}$, $\tilde{V}_1 \triangleq V_1 - \hat{V}_1 \in \mathbb{R}^{n \times N}$, $\tilde{V}_2 \triangleq V_2 - \hat{V}_2 \in \mathbb{R}^{n \times N}$ are the estimate mismatches for the ideal NN weights, and $O(\tilde{V}_1^{\mathrm{T}} x_d + \tilde{V}_2^{\mathrm{T}} \dot{x}_d)^2 \in \mathbb{R}^{N+1}$ is the higher-order term in the Taylor series of the vector functions σ_d in the neighborhood of $\hat{V}_1^{\mathrm{T}} x_d + \hat{V}_2^{\mathrm{T}} \dot{x}_d$ as

$$\sigma_d = \hat{\sigma}_d + \hat{\sigma}_d'(\tilde{V}_1^{\mathrm{T}} x_d + \tilde{V}_2^{\mathrm{T}} \dot{x}_d) + O(\tilde{V}_1^{\mathrm{T}} x_d + \tilde{V}_2^{\mathrm{T}} \dot{x}_d)^2 \tag{15}$$

Motivation for segregating the terms in Eqs. (10), (12), and (13) is derived from the fact that different terms have different bounds. The term $\tilde{N}_1$ includes all terms which can be upper bounded by states, whereas N includes all terms which can be upper bounded by constants. The difference between the terms N_D and N_B in Eq. (12) is that the first time derivative of N_D is upper-bounded by a constant, whereas the term $\dot{N}_B$ is state dependent. The term N_B is further segregated as Eq. (13) to aid in the weight update law design for the DNN in Eq. (7). In the subsequent stability analysis, the term N_{B_1} is canceled by the error feedback and the sliding mode term, while the term N_{B_2} is partially compensated for by the weight update laws and partially canceled by the error feedback and the sliding mode term.

Using Eqs. (3), (4), and Assumptions 4, 5, the proj$(\cdot)$ algorithm in Eq. (7) and the mean value theorem [24], the auxiliary function $\tilde{N}_1$ in Eq. (11) can be upper-bounded as

$$\|\tilde{N}_1\| \leq \zeta_1 \|z\| \tag{16}$$

where $\zeta_1 \in \mathbb{R}$ is a computable positive constant, and $z \in \mathbb{R}^{6n}$ is defined as

$$z \triangleq [\tilde{x}^{\mathrm{T}}\, e^{\mathrm{T}}\, r_{\mathrm{es}}^{\mathrm{T}}\, r_{\mathrm{tr}}^{\mathrm{T}}\, \nu^{\mathrm{T}}\, \eta^{\mathrm{T}}]^{\mathrm{T}} \tag{17}$$

Based on Assumptions 3–6, the Taylor series expansion in Eq. (15), and the weight update laws in Eq. (7), the following bounds can be developed:

$$\begin{aligned} &\|N_D\| \leq \zeta_2,\ \|N_{B_1}\| \leq \zeta_3,\ \|N_{B_2}\| \leq \zeta_4 \\ &\|\dot{N}_D\| \leq \zeta_5,\ \|\dot{N}_B\| \leq \zeta_6 + \zeta_7 \|z\| \end{aligned} \tag{18}$$

where $\zeta_i \in \mathbb{R}, i = 2, 3, \ldots, 7$, are computable positive constants.

4 Robust Adaptive Tracking Controller

The control objective is to force the system state to asymptotically track the desired trajectory x_d, despite uncertainties and disturbances in the system. Quantitatively, the objective is to regulate the filtered tracking controller r_{tr} to zero. Using Eqs. (2)–(4) and (8), the open-loop dynamics of the tracking error in Eq. (4) are expressed as

$$\begin{aligned} \dot{r}_{\mathrm{tr}} = &W^{\mathrm{T}} \sigma + Gu + \varepsilon + d - \ddot{x}_d + \alpha(r_{\mathrm{tr}} - \alpha e - \eta) \\ &-(k+\alpha) r_{\mathrm{es}} - \alpha\eta + \tilde{x} + e - \nu \end{aligned} \tag{19}$$

The control input u is designed as a composition of the DNN term, the estimated states $\hat{x}, \dot{\hat{x}}$, and the sliding mode term as

$$u = G^{-1}[\ddot{x}_d - \hat{W}^{\mathrm{T}} \hat{\sigma}_d - (k+\alpha)(\dot{\hat{e}} + \alpha \hat{e}) - \beta_2 \mathrm{sgn}(e+\nu)] \tag{20}$$

where $\beta_2 \in \mathbb{R}$ is a positive constant control gain, and the tracking error estimate $\hat{e} \in \mathbb{R}^n$ is defined as $\hat{e} \triangleq \hat{x} - x_d$. Based on the fact that the estimated states are measurable, the tracking error estimate $\hat{e}$ and its derivative $\dot{\hat{e}}$ are measurable; moreover, r_{tr} is related to r_{es} as

$$r_{\mathrm{tr}} = r_{\mathrm{es}} + \dot{\hat{e}} + \alpha \hat{e} \tag{21}$$

Adding and subtracting $W^{\mathrm{T}} \sigma_d + W^{\mathrm{T}} \hat{\sigma}_d$ and using Eqs. (19)–(21), the closed-loop error system becomes

$$\dot{r}_{\mathrm{tr}} = \tilde{N}_2 + N - k r_{\mathrm{tr}} - \beta_2 \mathrm{sgn}(e+\nu) - e \tag{22}$$

where the auxiliary function $\tilde{N}_2 \in \mathbb{R}^n$ is defined as

$$\tilde{N}_2 \triangleq W^{\mathrm{T}}(\sigma - \sigma_d) - (\alpha^2 - 2)e - \nu + \tilde{x} - 2\alpha\eta \tag{23}$$

and the function N is introduced in Eq. (12). Similarly, using Eqs. (3), (4), Assumptions 4, 5, the proj$(\cdot)$ algorithm in Eq. (7), and mean value theorem [24], the auxiliary function $\tilde{N}_2$ in Eq. (23) can be upper-bounded as

$$\|\tilde{N}_2\| \leq \zeta_8 \|z\| \tag{24}$$

where $\zeta_8 \in \mathbb{R}$ is a computable positive constant.

To facilitate the subsequent stability analysis, let $y \in \mathbb{R}^{6n+2}$ be defined as $y \triangleq [z^{\mathrm{T}} \quad \sqrt{P} \quad \sqrt{Q}]^{\mathrm{T}}$ where the auxiliary function $P \in \mathbb{R}$ is the Filippov solution to the differential equation

$$\begin{aligned} \dot{P} &\triangleq L \\ P_0 &= \beta_1 \sum_{j=1}^{n} |\tilde{x}_j(0) + \nu_j(0)| + \beta_2 \sum_{j=1}^{n} |e_j(0) + \nu_j(0)| \\ &\quad - (\tilde{x}(0) + e(0) + 2\nu(0))^{\mathrm{T}} N(0) \end{aligned} \tag{25}$$

where the subscript $j = 1, 2, .., n$ denotes the jth element of $\tilde{x}(0)$, $e(0)$, or $\nu(0)$, and the auxiliary term $L \in \mathbb{R}$ is defined as

$$\begin{aligned} L \triangleq &- r_{\mathrm{es}}^{\mathrm{T}}(N_D + N_{B_1} - \beta_1 \mathrm{sgn}(\tilde{x} + \nu)) \\ &- r_{\mathrm{tr}}^{\mathrm{T}}(N_D + N_{B_1} - \beta_2 \mathrm{sgn}(e + \nu)) \\ &- (\dot{\tilde{x}} + \dot{e} + 2\dot{\nu})^{\mathrm{T}} N_{B_2} + \beta_3 \|z\|^2 \end{aligned} \tag{26}$$

where β_1, β_2 are introduced in Eqs. (6) and (20), and $\beta_3 \in \mathbb{R}$ is a positive constant. The control gains β_i, $i = 1, 2, 3$ are selected according to the sufficient conditions

$$\begin{aligned} &\beta_1, \beta_2 > \max\left(\zeta_2 + \zeta_3 + \zeta_4, \zeta_2 + \zeta_3 + \frac{\zeta_5}{\alpha} + \frac{\zeta_6}{\alpha}\right) \\ &\beta_3 > 2\zeta_7 \end{aligned} \tag{27}$$

where ζ_i, $i = 1, 2, \ldots, 7$ are introduced in Eqs. (16) and (18). Provided the sufficient conditions in Eq. (27) are satisfied, the following inequality can be obtained $P \geq 0$ (see Ref. [25]). The auxiliary function $Q \in \mathbb{R}$ is defined as

$$Q \triangleq \frac{\alpha}{2}\left[\mathrm{tr}\left(\tilde{W}^{\mathrm{T}} \Gamma_w^{-1} \tilde{W}\right) + \mathrm{tr}\left(\tilde{V}_1^{\mathrm{T}} \Gamma_{v1}^{-1} \tilde{V}_1\right) + \mathrm{tr}\left(\tilde{V}_2^{\mathrm{T}} \Gamma_{v2}^{-1} \tilde{V}_2\right)\right] \tag{28}$$

where $\mathrm{tr}(\cdot)$ denotes the trace of a matrix. Since the gains $\Gamma_w, \Gamma_{v1}, \Gamma_{v2}$ are symmetric, positive-definite matrices, $Q \geq 0$.

5 Lyapunov Stability Analysis for Dynamic Neural Network-Based Observation and Control

THEOREM 1. *The DNN-based observer and controller proposed in Eqs. (6) and (20), respectively, along with the weight update laws in Eq. (7) ensure asymptotic estimation and tracking in sense that*

$$\|\dot{\tilde{x}}\| \to 0 \text{ as } t \to \infty, \text{ and } \|e\| \to 0 \text{ as } t \to \infty$$

provided the gain conditions in Eq. (27) are satisfied, and the control gains α and $k = k_1 + k_2$ introduced in Eqs. (4) and (5) are selected as

$$\lambda \triangleq \min(\alpha, k_1) > \frac{\zeta_1^2 + \zeta_8^2}{4k_2} + \beta_3 \tag{29}$$

where $\zeta_1, \zeta_8, \beta_3$ are introduced in Eqs. (16), (24), and (26), respectively.

Proof. Consider the Lyapunov candidate function $V_L : \mathcal{D} \to \mathbb{R}$, which is a Lipschitz continuous positive definite function defined as

$$V_L \triangleq \frac{1}{2}\tilde{x}^{\mathrm{T}}\tilde{x} + \frac{1}{2}e^{\mathrm{T}}e + \frac{1}{2}\nu^{\mathrm{T}}\nu + \frac{1}{2}\eta^{\mathrm{T}}\eta + \frac{1}{2}r_{\mathrm{es}}^{\mathrm{T}}r_{\mathrm{es}} + \frac{1}{2}r_{\mathrm{tr}}^{\mathrm{T}}r_{\mathrm{tr}} + P + Q \tag{30}$$

which satisfies the following inequalities:

$$\frac{1}{2}||y||^2 \le V_L \le ||y||^2 \tag{31}$$

Let $\dot{y} = h$ represent the closed-loop differential equations in Eqs. (4)–(7), (8), (10), (22), and (25), where $h \in \mathbb{R}^{6n+2}$ denotes the right-hand side of the closed-loop error signals. Using Filippov's theory of differential inclusions [26–29], the existence of solutions can be established for $\dot{y} \in K[h](y)$, where $K[h] \triangleq \cap_{\delta>0} \cap_{\mu M=0} \overline{co}\, h(B(y,\delta) - M)$, where $\cap_{\mu M=0}$ denotes the intersection of all sets M of Lebesgue measure zero, $\overline{co}$ denotes convex closure, and $B(y,\delta) = \{w \in R^{6n+2} \,|\, ||y - w|| < \delta\}$. The generalized time derivative of Eq. (30) exists almost everywhere (a.e.), i.e., for almost all $t \in [t_0, t_f]$, and $\dot{V}_L \in^{a.e.} \dot{\tilde{V}}_L$, where $\dot{\tilde{V}}_L = \cap_{\xi \in \partial V_L(y)} \xi^{\mathrm{T}} K[\Psi]^{\mathrm{T}}$, ∂V_L is the generalized gradient of V_L [30], and $\Psi \triangleq [\dot{\tilde{x}}^{\mathrm{T}}\, \dot{e}^{\mathrm{T}}\, \dot{\nu}^{\mathrm{T}}\, \dot{\eta}^{\mathrm{T}}\, \dot{r}_{\mathrm{es}}^{\mathrm{T}}\, \dot{r}_{\mathrm{tr}}^{\mathrm{T}} (1/2)P^{-(1/2)}\dot{P}(1/2)Q^{-(1/2)}\dot{Q}]$. Since V_L is continuously differentiable, $\dot{\tilde{V}}_L$ can be simplified as [31]

$$\dot{\tilde{V}}_L = \nabla V^{\mathrm{T}} K \Psi^{\mathrm{T}} = \left[\tilde{x}^{\mathrm{T}}\, e^T\, \nu^T\, \eta^T\, r_{\mathrm{es}}^{\mathrm{T}}\, r_{\mathrm{tr}}^{\mathrm{T}}\, 2P^{\frac{1}{2}}\, 2Q^{\frac{1}{2}}\right] K \Psi^T$$

Using the calculus for $K[\cdot]$ from Ref. [32] (Theorem 1; Properties 2, 5, 7), and substituting the dynamics from Eqs. (4), (5), (8), (10), (22), (25), (26), and (28), $\dot{\tilde{V}}_L$ can be rewritten as

$$\begin{aligned}
\dot{\tilde{V}}_L \subset\; & \tilde{x}^{\mathrm{T}}(r_{\mathrm{es}} - \alpha\tilde{x} - \eta) + e^{\mathrm{T}}(r_{\mathrm{tr}} - \alpha e - \eta) \\
& + \eta^{\mathrm{T}}[-(k+\alpha)r_{\mathrm{es}} - \alpha\eta + \tilde{x} + e - \nu] \\
& + \nu^{\mathrm{T}}(\eta - \alpha\nu) + r_{\mathrm{es}}^{\mathrm{T}}\{(k+\alpha)\eta - \tilde{x}\} \\
& + r_{\mathrm{es}}^{\mathrm{T}}\{\tilde{N}_1 + N - kr_{\mathrm{es}} - \beta_1 K[\mathrm{sgn}(\tilde{x} + \nu)]\} \\
& + r_{\mathrm{tr}}^{\mathrm{T}}\{\tilde{N}_2 + N - kr_{\mathrm{tr}} - \beta_2 K[\mathrm{sgn}(e + \nu)] - e\} \\
& - r_{\mathrm{es}}^{\mathrm{T}}\{N_D + N_{B_1} - \beta_1 K[\mathrm{sgn}(\tilde{x} + \nu)]\} \\
& - r_{\mathrm{tr}}^{\mathrm{T}}\{N_D + N_{B_1} - \beta_2 K[\mathrm{sgn}(e + \nu)]\} + \beta_3||z||^2 \\
& - (\dot{\tilde{x}} + \dot{e} + 2\dot{\nu})^{\mathrm{T}} N_{B_2} - \alpha tr(\tilde{W}^{\mathrm{T}}\Gamma_w^{-1}\dot{\hat{W}}) \\
& - \alpha tr(\tilde{V}_1^{\mathrm{T}}\Gamma_{v1}^{-1}\dot{\hat{V}}_1) - \alpha tr(\tilde{V}_2^{\mathrm{T}}\Gamma_{v2}^{-1}\dot{\hat{V}}_2)
\end{aligned} \tag{32}$$

Using the fact that $K[\mathrm{sgn}(\tilde{x} + \nu)] = \mathrm{SGN}(\tilde{x} + \nu)$ [32], such that $\mathrm{SGN}(\tilde{x}_i + \nu_i) = 1$ if $(\tilde{x}_i + \nu_i) > 0$, $[-1, 1]$ if $(\tilde{x}_i + \nu_i) = 0$, and -1 if $(\tilde{x}_i + \nu_i) < 0$ (the subscript i denotes the ith element), the set in Eq. (32) reduces to the scalar inequality, since the right-hand side is continuous a.e., i.e., the right-hand side is continuous except for the Lebesgue measure zero set of times when[1] $r_{\mathrm{es}}^{\mathrm{T}}\mathrm{SGN}(\tilde{x} + \nu) - r_{\mathrm{es}}^{\mathrm{T}}\mathrm{SGN}(\tilde{x} + \nu) = 0$. The fact that $r_{\mathrm{tr}}^{\mathrm{T}}\mathrm{SGN}(e + \nu) - r_{\mathrm{tr}}^{\mathrm{T}}\mathrm{SGN}$ $(e + \nu) = 0$ can be achieved similarly. Substituting the weight update laws in Eq. (7) and canceling common terms yields

$$\begin{aligned}
\dot{\tilde{V}}_L \overset{a.e.}{\le} & -\alpha\tilde{x}^{\mathrm{T}}\tilde{x} - \alpha e^{\mathrm{T}}e - \alpha\nu^{\mathrm{T}}\nu - \alpha\eta^{\mathrm{T}}\eta - kr_{\mathrm{es}}^{\mathrm{T}}r_{\mathrm{es}} \\
& - kr_{\mathrm{tr}}^{\mathrm{T}}r_{\mathrm{tr}} + r_{\mathrm{es}}^{\mathrm{T}}\tilde{N}_1 + r_{\mathrm{tr}}^{\mathrm{T}}\tilde{N}_2 + \beta_3||z||^2
\end{aligned} \tag{33}$$

Using Eqs. (16) and (24), substituting $k = k_1 + k_2$, and completing the squares, the expression in Eq. (33) can be further bounded as

$$\begin{aligned}
\dot{\tilde{V}}_L & \overset{a.e.}{\le} -\alpha||\tilde{x}||^2 - \alpha||e||^2 - \alpha||\nu||^2 - \alpha||\eta||^2 - k_1||r_{\mathrm{es}}||^2 \\
& \quad - k_1||r_{\mathrm{tr}}||^2 + \left(\frac{\zeta_1^2 + \zeta_8^2}{4k_2} + \beta_3\right)||z||^2 \\
& \overset{a.e.}{\le} -\left(\lambda - \frac{\zeta_1^2 + \zeta_8^2}{4k_2} - \beta_3\right)||z||^2 \overset{a.e.}{\le} -c||z||^2
\end{aligned} \tag{34}$$

for some positive constant c, and λ is defined in Eq. (29). The inequalities in Eqs. (31) and (34) show that $V_L \in \mathcal{L}_\infty$; hence, $\tilde{x}$, e, ν, η, r_{es}, r_{tr}, P, and $Q \in \mathcal{L}_\infty$. Using Eq. (4), it can be shown that $\dot{\tilde{x}}$, $\dot{e} \in \mathcal{L}_\infty$. Based on the assumption that x_d, $\dot{x}_d \in \mathcal{L}_\infty$, and e, $\dot{e} \in \mathcal{L}_\infty$, x, $\dot{x} \in \mathcal{L}_\infty$ by Eq. (3); moreover, using Eq. (3) and $\tilde{x}$, $\dot{\tilde{x}} \in \mathcal{L}_\infty$, $\hat{x}$, $\dot{\hat{x}} \in \mathcal{L}_\infty$. Based on Assumptions 2 and 5, the projection algorithm in Eq. (7), the boundedness of the sgn and σ functions, and x_d, $\dot{x}_d$, $\hat{x}$, $\dot{\hat{x}} \in \mathcal{L}_\infty$, the control input u is bounded from Eq. (20). Similarly, $\dot{\nu}$, $\dot{\eta}$, $\dot{r}_{\mathrm{es}}$, $\dot{r}_{\mathrm{tr}} \in \mathcal{L}_\infty$ by using Eqs. (5), (8), (9), (22); hence $\dot{z} \in \mathcal{L}_\infty$, using Eq. (17); hence, z is uniformly continuous. From Eq. (34), Ref. [33, Corollary 1] can be invoked to show that $c||z||^2 \to 0$ as $t \to \infty$. Using the definition of z in Eq. (17), it can be shown that $||\tilde{x}||, ||e||, ||r_{\mathrm{es}}||, ||r_{\mathrm{tr}}||, ||\nu||, ||\eta|| \to 0$ as $t \to \infty$. Using Eq. (4), and standard linear analysis, it can be further shown that $||\dot{\tilde{x}}|| \to 0$ as $t \to \infty$. □

6 Experiment Results

The performance of the output feedback control method is tested on a two-link robot manipulator, where two aluminum links are mounted on a 240 N·m (first link) and a 20 N·m (second link) switched reluctance motor. The motor resolvers provide rotor position measurements with a resolution of 614,400 pulses/revolution. Data acquisition and control implementation were performed in real-time using QNX at a frequency of 1.0 kHz. The two-link revolute robot is modeled with the following dynamics:

$$M\ddot{x} + V_m\dot{x} + F + \tau_d = u \tag{35}$$

where $x = [x_1 \quad x_2]^{\mathrm{T}}$ are the angular positions (rad), $\dot{x} = [\dot{x}_1 \quad \dot{x}_2]^{\mathrm{T}}$ are the angular velocities (rad/s) of the two links, respectively, $M \in \mathbb{R}^{2\times2}$ is the inertia matrix, $V_m \in \mathbb{R}^{2\times2}$ denotes the centripetal-Coriolis matrix, $F \in \mathbb{R}^2$ denotes friction, and $\tau_d \in \mathbb{R}^2$ is the external disturbance. The system in Eq. (35) can be rewritten as $\ddot{x} = f + Gu + d$, where f and G are defined as $f \triangleq -M^{-1}(V_m\dot{x} + F)$, $G(x) \triangleq M^{-1}$. The desired trajectory for each link of the manipulator is given as (in degrees) $x_{1d} = 30\sin(1.5t)(1 - \exp(-0.01t^3))$, $x_{2d} = 30\sin(2.0t)(1 - \exp(-0.05t^3))$. The control gains are chosen as $k = \mathrm{diag}(25, 90)$, $\alpha = \mathrm{diag}(22, 30)$, $\beta_1 = \beta_2 = 0.2$, and $\Gamma_w = 0.2\mathbb{I}_{8\times8}$, $\Gamma_{v1} = \Gamma_{v2} = 0.2\mathbb{I}_{2\times2}$, where $\mathbb{I}_{n\times n}$ denotes an identity matrix of appropriate dimensions. The NNs was implemented with seven hidden layer neurons, and the neural network weights are initialized as uniformly distributed random numbers in the interval $[0.1, 0.3]$. The initial conditions of the system and the observer were selected as $x = \dot{x} = [0\,0]^{\mathrm{T}}$, and $\hat{x} = \dot{\hat{x}} = [0\,0]^{\mathrm{T}}$, respectively.

The Lyapunov-based analysis provides conservative sufficient gain conditions. The control gains for the experiments were obtained by choosing gains and then adjusting them based on the transient and steady-state performance. If the response exhibited a

[1] Let $\Phi \triangleq \tilde{x} + \nu$ The set of times $\Lambda \triangleq \{t \in [0,\infty) : r_{\mathrm{es}}(t)^T K[\mathrm{sgn}(\Phi(t))] - r_{\mathrm{es}}(t)^T K[\mathrm{sgn}(\Phi(t))] \ne \{0\}\}$ is equal to the set of times $\{t : \Phi(t) = 0 \wedge r_{\mathrm{es}}(t) \ne 0\}$ Using the fact that $\eta = \dot{\nu} + \alpha\nu$, res can be expressed as $r_{\mathrm{es}} = \dot{\Phi} + \alpha\Phi$ Thus, the set Λ can also be represented by $\{t : \Phi(t) = 0 \wedge \dot{\Phi}(t) \ne 0\}$ Since $\phi : [0,\infty) \to \mathbb{R}^n$ is continuously differentiable, it can be shown that the set of time instances $\{t : \Phi(t) = 0 \wedge \dot{\Phi}(t) \ne 0\}$ is isolated, and thus, measure zero; hence, Λ is measure zero.

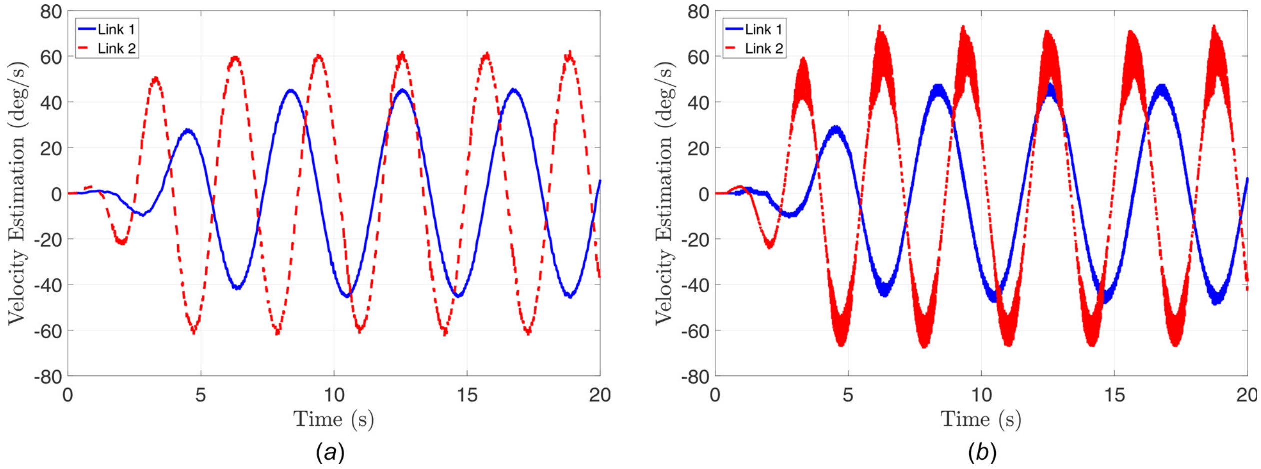

Fig. 1 Velocity estimation $\dot{x}(t)$ using (*a*) DNN-based observer and (*b*) numerical backwards difference: (*a*) velocity estimation by DNN observer and (*b*) velocity estimation by backwards difference

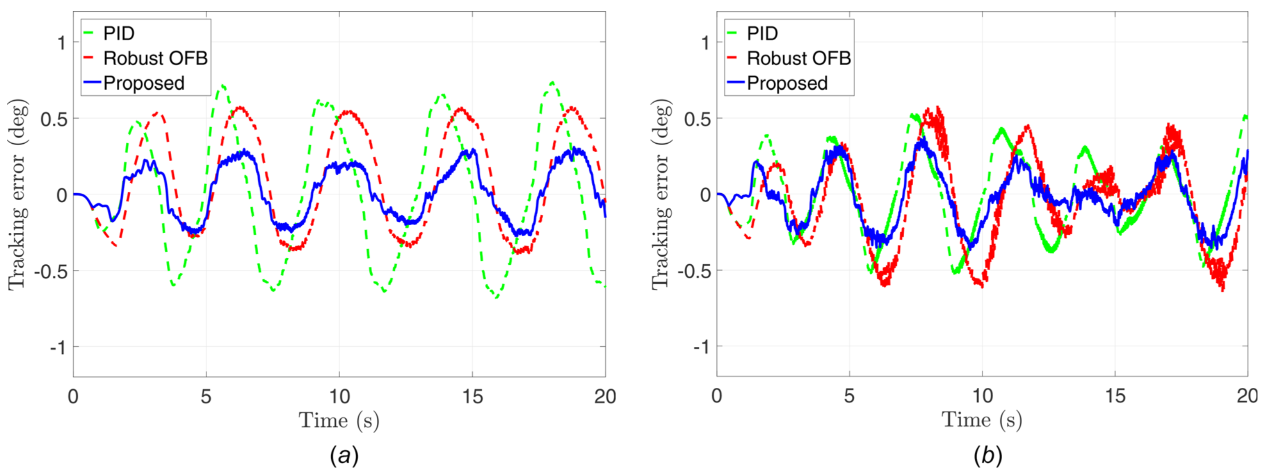

Fig. 2 The tracking errors $e(t)$ of (*a*) link 1 and (*b*) link 2 using classical PID, robust discontinuous OFB controller [15], and proposed controller: (*a*) link 1 tracking error and (*b*) link 2 tracking error

prolonged transient response (compared with the response obtained with other gains), the proportional gains were adjusted. If the response exhibited overshoot, derivative gains were adjusted. The control gains for the experiments were tuned based on this trial and error basis. In contrast to this trial and error approach, the control gains could have been adjusted using more methodical approaches as described in various survey papers on the topic [34,35].

The performance of the proposed output feedback controller is compared with two controllers: a classical PID controller and the discontinuous OFB controller in Ref. [15]. A standard backward difference algorithm is used to numerically determine velocity from the encoder readings to implement the PID controller. Control gains for the discontinuous controller in Ref. [15] were selected as $K_1 = 0.2$, $K_2 = \mathrm{diag}(410,\ 38)$, and control gains for the PID controller were selected as $K_d = \mathrm{diag}(120,\ 30),\ K_p = \mathrm{diag}(750,\ 90)$, and $K_i = \mathrm{diag}(650,\ 100)$. The DNN-based observer yields better velocity estimation in comparison with the high frequency content results from a backward difference method as depicted in Fig. 1. Moreover, the tracking errors and control torques for all controllers are illustrated in Figs. 2 and 3, respectively. Table 1 shows the root-mean-square (RMS) and peak tracking errors and torques of Links 1 and 2 at steady-state for all methods. The developed controller is shown to exhibit lower tracking errors with less control authority than the comparative controllers. Hence, the experiments illustrate that using the velocity estimation from a DNN-based observer, which adaptively compensates for unknown uncertainties in the system, results in improved control performance with lower frequency content than the compared methods. To illustrate the lower frequency response of the proposed method compared to Ref. [15] and the PID controller, the frequency analysis plots of the experiment results are shown in Fig. 4. The high frequency content in the velocity estimation of the backward difference method results in the highest frequency content in control torques of PID controller. The proposed method is a robust adaptive controller with a DNN structure to learn the system uncertainties to asymptotically observe the unmeasurable state and asymptotically track the desired trajectory. On the other hand, the OFB control method in Ref. [15] is a purely robust feedback method, where all uncertainties are damped out by a sliding mode term resulting in higher frequency control torques than the proposed adaptive control method, as seen in experiment results.

7 Conclusion

A DNN observer-based output feedback control of a class of second-order nonlinear uncertain systems is developed. The DNN-based observer works in conjunction with a dynamic filter to estimate the unmeasurable state. The DNN is updated online by weight update laws based on the estimation error, tracking error, and filter output. The controller is a combination of the NN feedforward term, and the estimated state feedback and sliding mode terms. Asymptotic estimation of the unmeasurable state and

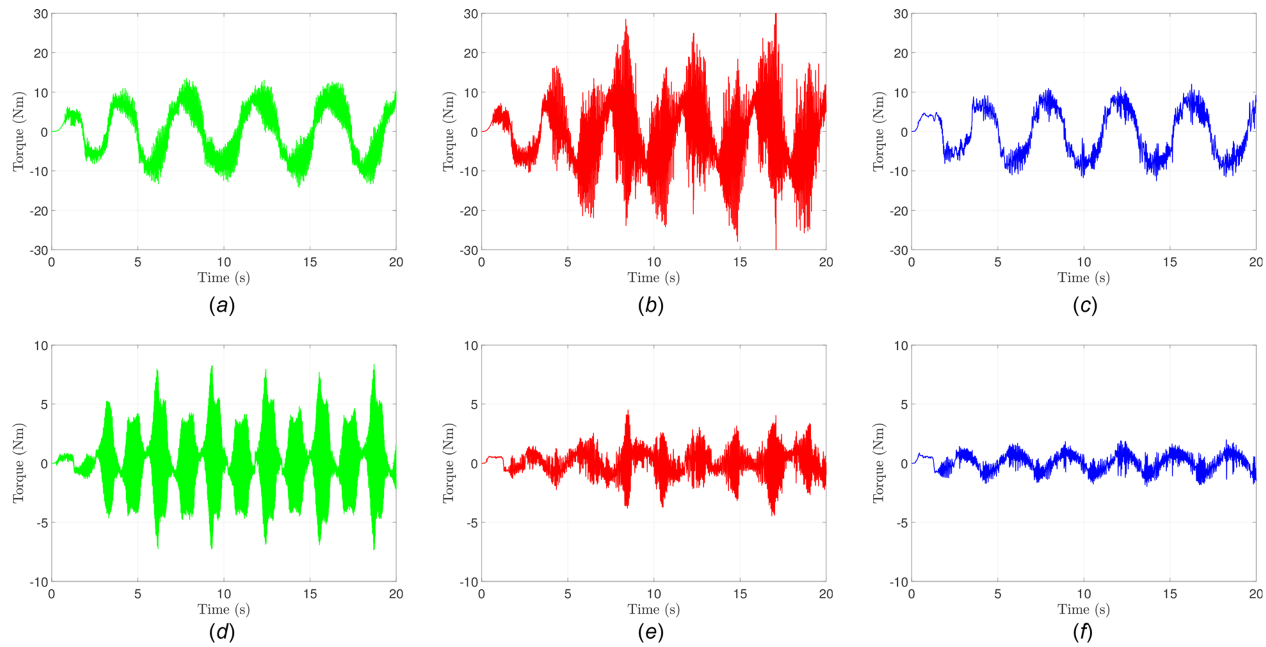

Fig. 3 The control inputs for link 1 and link 2 using (*a*), (*d*) classical PID, (*b*), (*e*) robust discontinuous OFB controller [15], and (*c*), (*f*) proposed controller: (*a*) link 1 control input (PID controller), (*b*) link 1 control input (robust OFB controller), (*c*) link 1 control input (proposed), (*d*) link 2 control input (PID controller), (*e*) link 2 control input (robust OFB controller), and (*f*) link 2 control input (proposed)

Table 1 Steady-state RMS errors and torques for each of the analyzed control designs

	SSRMS e_1	SSRMS e_2	Max $\|e_1\|$	Max $\|e_2\|$	SSRMS τ_1	SSRMS τ_2	Max $\|\tau_1\|$	Max $\|\tau_2\|$
Classical PID	0.4538	0.2700	0.7371	0.5267	6.5805	2.4133	14.5871	9.0015
Robust OFB [15]	0.3552	0.2947	0.5819	0.6429	8.6509	1.2585	56.5796	4.6107
Proposed	0.1743	0.1740	0.3100	0.3760	6.3484	0.6944	12.5562	2.2122

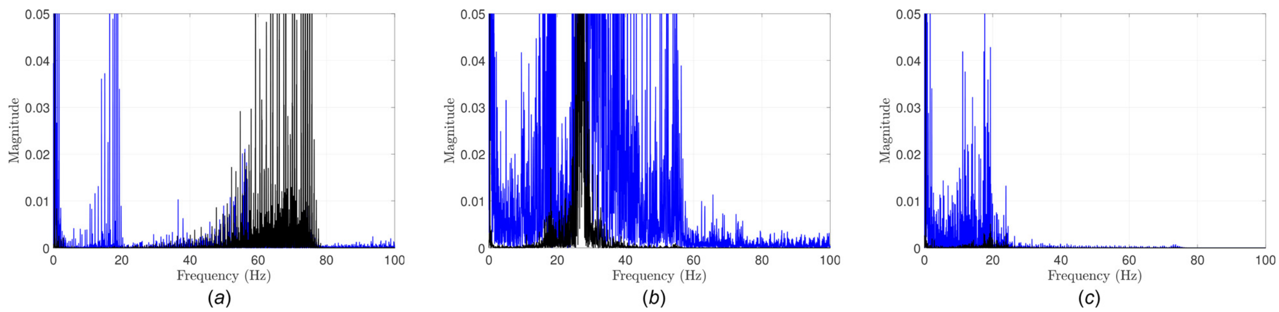

Fig. 4 Frequency analysis of torques *u*(*t*) using (*a*) classical PID and (*b*) robust discontinuous OFB controller [15], and (*c*) proposed controller: (*a*) frequency analysis (PID controller), (*b*) frequency analysis (robust OFB controller), and (*c*) frequency analysis (proposed)

asymptotic tracking results are achieved, simultaneously. Results from an experiment using a two-link robot manipulator demonstrate the performance of the proposed output feedback controller.

Acknowledgment

This research was supported in part by NSF award numbers 0547448, 0901491, 1161260, and 1217908.

References

[1] Berghuis, H., and Nijmeijer, H., 1993, "A Passivity Approach to Controller-Observer Design for Robots," IEEE Trans. Robot. Autom., **9**(6), pp. 740–754.

[2] Do, K. D., Jiang, Z., and Pan, J., 2004, "A Global Output-Feedback Controller for Simultaneous Tracking and Stabilization for Unicycle-Type Mobile Robots," IEEE Trans. Robot. Autom., **20**(3), pp. 589–594.

[3] Lim, S. Y., Dawson, D. M., and Anderson, K., 1996, "Re-Examining the Nicosia–Tomei Robot Observer-Controller for a Backstepping Perspective," IEEE Trans. Control Syst. Technol., **4**(3), pp. 304–310.

[4] Ordaz, P., Espinoza, E. S., and Munoz, F., 2014, "Global Stability of PD+ Controller With Velocity Estimation," 53rd IEEE Conference on Decision and Control, Dec. 15–17, pp. 2585–2590.

[5] Arteaga, M. A., and Kelly, R., 2004, "Robot Control Without Velocity Measurements: New Theory and Experiment Results," IEEE Trans. Robot. Autom., **20**(2), pp. 297–308.

[6] Kaneko, K., and Horowitz, R., 1997, "Repetitive and Adaptive Control of Robot Manipulators With Velocity Estimation," IEEE Trans. Robot. Autom., **13**(2), pp. 204–217.

[7] Burg, T., Dawson, D. M., and Vedagarbha, P., 1997, "A Redesigned Dcal Controller Without Velocity Measurements: Theory and Demonstration," Robotica, **15**(4), pp. 337–346.
[8] Kim, Y. H., and Lewis, F. L., 1999, "Neural Network Output Feedback Control of Robot Manipulators," IEEE Trans. Robot. Autom., **15**(2), pp. 301–309.
[9] Patino, H. D., and Liu, D., 2000, "Neural Network-Based Model Reference Adaptive Control System," IEEE Trans. Syst., Man, Cybern., Part B, **30**(1), pp. 198–204.
[10] Seshagiri, S., and Khalil, H., 2000, "Output Feedback Control of Nonlinear Systems Using RBF Neural Networks," IEEE Trans. Neural Network, **11**(1), pp. 69–79.
[11] Choi, J. Y., and Farrell, J. A., 2001, "Adaptive Observer Backstepping Control Using Neural Network," IEEE Trans. Neural Network, **12**(5), pp. 1103–1112.
[12] Calise, A. J., Hovakimyan, N., and Idan, M., 2001, "Adaptive Output Feedback Control of Nonlinear Systems Using Neural Networks," Automatica, **37**(8), pp. 1201–1211.
[13] Hovakimyan, N., Nardi, F., Calise, A., and Kim, N., 2002, "Adaptive Output Feedback Control of Uncertain Nonlinear Systems Using Single-Hidden-Layer Neural Networks," IEEE Trans. Neural Networks, **13**(6), pp. 1420–1431.
[14] Islam, S., and Liu, P., 2011, "Robust Adaptive Fuzzy Output Feedback Control System for Robot Manipulators," IEEE/ASME Trans. Mechatron., **16**(2), pp. 288–296.
[15] Xian, B., de Queiroz, M. S., Dawson, D. M., and McIntyre, M., 2004, "A Discontinuous Output Feedback Controller and Velocity Observer for Nonlinear Mechanical Systems," Automatica, **40**(4), pp. 695–700.
[16] Dinh, H. T., Bhasin, S., Kim, D., and Dixon, W. E., 2012, "Dynamic Neural Network-Based Global Output Feedback Tracking Control for Uncertain Second-Order Nonlinear Systems," American Control Conference, Montréal, Canada, June 27–29, pp. 6418–6423.
[17] Polycarpou, M., and Ioannou, P., 1991, "Identification and Control of Nonlinear Systems Using Neural Network Models: Design and Stability Analysis," Systems Report, University of Southern California, Los Angeles, CA, Tech. Report No. 91-09-01.
[18] Hornick, K., 1991, "Approximation Capabilities of Multilayer Feedforward Networks," Neural Networks, **4**(2), pp. 251–257.
[19] Lewis, F. L., Selmic, R., and Campos, J., 2002, *Neuro-Fuzzy Control of Industrial Systems With Actuator Nonlinearities*, Society for Industrial and Applied Mathematics, Philadelphia, PA.
[20] Funahashi, K., and Nakamura, Y., 1993, "Approximation of Dynamic Systems by Continuous-Time Recurrent Neural Networks," Neural Networks, **6**(6), pp. 801–806.
[21] Gupta, M., Jin, L., and Homma, N., 2003, *Static and Dynamic Neural Networks: From Fundamentals to Advanced Theory*, Wiley, Hoboken, NJ.
[22] Dixon, W. E., Behal, A., Dawson, D. M., and Nagarkatti, S., 2003, *Nonlinear Control of Engineering Systems: A Lyapunov-Based Approach*, Birkhauser, Boston, MA.
[23] Krstic, M., Kokotovic, P. V., and Kanellakopoulos, I., 1995, *Nonlinear and Adaptive Control Design*, Wiley, New York.
[24] Xian, B., Dawson, D. M., de Queiroz, M. S., and Chen, J., 2004, "A Continuous Asymptotic Tracking Control Strategy for Uncertain Nonlinear Systems," IEEE Trans. Autom. Control, **49**(7), pp. 1206–1211.
[25] Dinh, H., Bhasin, S., and Dixon, W. E., 2010, "Dynamic Neural Network-Based Robust Identification and Control of a Class of Nonlinear Systems," IEEE Conference on Decision Control, Atlanta, GA, Dec. 15–17, pp. 5536–5541.
[26] Filippov, A., 1964, "Differential Equations With Discontinuous Right-Hand Side," Am. Math. Soc. Transl., **42**(2), pp. 199–231.
[27] Filippov, A. F., 1988, *Differential Equations With Discontinuous Right-Hand Sides*, Kluwer Academic Publishers, Dordrecht, The Netherlands.
[28] Smirnov, G. V., 2002, *Introduction to the Theory of Differential Inclusions*, Vol. 41, American Mathematical Society, Providence, RI.
[29] Aubin, J. P., and Frankowska, H., 2009, *Set-Valued Analysis*, Birkhäuser, Boston, MA.
[30] Clarke, F. H., 1990, *Optimization and Nonsmooth Analysis*, SIAM, New York.
[31] Shevitz, D., and Paden, B., 1994, "Lyapunov Stability Theory of Nonsmooth Systems," IEEE Trans. Autom. Control, **39**(9), pp. 1910–1914.
[32] Paden, B., and Sastry, S., 1987, "A Calculus for Computing Filippov's Differential Inclusion With Application to the Variable Structure Control of Robot Manipulators," IEEE Trans. Circuits Syst., **34**(1), pp. 73–82.
[33] Fischer, N., Kamalapurkar, R., and Dixon, W. E., 2013, "Lasalle-Yoshizawa Corollaries for Nonsmooth Systems," IEEE Trans. Automat. Control, **58**(9), pp. 2333–2338.
[34] Killingsworth, N. J., and Krstic, M., 2006, "PID Tuning Using Extremum Seeking: Online, Model-Free Performance Optimization," IEEE Control Syst. Mag., **26**(1), pp. 70–79.
[35] Aström, K., Hägglund, T., Hang, C., and Ho, W., 1993, "Automatic Tuning and Adaptation for PID Controllers—A Survey," Control Eng. Pract., **1**(4), pp. 669–714.